Theor Chim Acta (1992) 82: 57–73

Theoretica
Chimica Acta

Angle and bond-length dependent C_6 coefficients for H_2 interacting with H, Li, Be and rare gas atoms

Ajit J. Thakkar[1], Zhe-Ming Hu[1,]*, Claudio E. Chuaqui[2], J. Scott Carley[2], and Robert J. LeRoy[2]

Centres of Excellence for Molecular and Interfacial Dynamics

[1] Department of Chemistry, University of New Brunswick, Fredericton, New Brunswick E3B 5A3, Canada

[2] Guelph-Waterloo Centre for Graduate Work in Chemistry, University of Waterloo, Waterloo, Ontario N2L 3G1, Canada

Received December 20, 1990; received in revised form February 28, 1991/Accepted May 20, 1991

Summary. Accurate new C_6 dispersion energy coefficients, and their dependence on the diatom orientation and bond length, are calculated for molecular hydrogen interacting with an atom of H, Li, Be, He, Ne, Ar, Kr or Xe. They are generated from accurate *ab initio* pseudo dipole oscillator strength distributions (DOSD) for H_2, H, He and Be, and reliable semiempirical ones for Li, Ne, Ar, Kr and Xe. Compact power series expansions for the diatom bond-length dependence of these coefficients, suitable for incorporation into representations of full potential energy surfaces for these systems, are determined and assessed.

Key words: C_6 – Dispersion energy – H_2-(rare gas) – H_2–Li – H_2–Be – H_2–H

1. Introduction

The dominant contribution to the long-range interaction between non-polar species is the induced dipole-induced dipole or London dispersion energy. In second-order perturbation theory, neglect of electron overlap between the interacting species leads to a simple inverse-power form for this energy, C_6/R^6, where C_6 is a constant determined by the properties of the isolated component species and R is the intermolecular distance [1, 2]. However, in spite of its substantial influence on many experimental properties, competition from higher inverse-power contributions to the long-range potential and the "damping" effect of non-negligible electron overlap make it difficult to determine accurate values of these coefficients from experimental data [3–5]. At the same time, the quality of potential energy function determined from fits to experimental data, particularly for weak Van der Waals interactions, can be as sensitive to the form chosen for the potential as to the actual details of fit. Thus, the determination of accurate theoretical C_6 coefficients for incoporation into model potentials is a matter of considerable importance and urgency.

---

* *Present address*: Department of Chemistry, McGill University, Montréal, Québec H3A 2K6, Canada

A dramatic illustration of this need for accurate theoretical C_6 coefficients is provided by the history of the experimentally determined potential energy surfaces for the molecular hydrogen-rare gas systems. The first empirical three-dimensional potential energy surface for this (or any other) atom-diatom Van der Waals system was based on Lennard–Jones (12,6) radial strength functions whose parameters were determined [6] from least-squares fits to discrete spectroscopic data [7]. While that potential function accounted accurately for all of the infrared transition frequencies for both H_2– and D_2–Ar, as well as for independent elastic differential scattering cross-section measurements [8, 9], its predictions were in marked disagreement with the observed "glory" structure in the low energy integral scattering cross-sections [10]. However, when a more flexible potential energy surface which incorporated a bond-length dependent and anisotropic theoretical C_6 term was fitted to those *same* spectroscopic data, yielding the *same* overall quality of fit [9], the more realistic radial form imposed by the theoretical C_6 coefficients led to virtually exact agreement with those integral cross sections [11, 12].

In general, the second-order induced dipole-induced dipole dispersion energy for the interaction between an S-state atom and a homonuclear diatomic molecule in a Σ electronic state may be written as [1, 2]:

$$E_{am}^{(2)}(R, r, \theta) = -C_6(r, \theta)/R^6 = -[C_6^0(r) + C_6^2(r)P_2(\cos\theta)]/R^6 \tag{1}$$

where r is the bond length of the diatom, θ the angle between the diatom axis and a vector from its centre of mass to the atom, and $P_2(\cos\theta)$ the usual second-order Legendre polynomial. The present paper addresses the problem of determining and representing $C_6^0(r)$ and $C_6^2(r)$ for the interactions of molecular hydrogen with rare gas atoms and with atomic H, Li and Be.

Estimates of these coefficients computed from semiempirical pseudo dipole oscillator strength distributions (pseudo-DOSD) were reported by Victor and coworkers [13] for ground-state H_2 interacting with a variety of atoms, including all of those treated here. For these same interactions (excluding H_2–Be), Langhoff et al. [14] reported bounds for C_6^0 and estimates of C_6^2 calculated from Padé approximants to dynamic polarizabilities based upon semiempirical Cauchy moments of the DOSD. However, neither of those studies treated the dependence of the dispersion coefficients on the bond length of the diatom. That was first done by Meyer and coworkers [15, 16] (see also Thakkar [17]), who calculated *ab initio* values of the H_2–He and H_2–H_2 dispersion coefficients for three different values of the H_2 bond length, and then performed an approximate average over the zero-point motion of the diatom.

In an initial effort to obtain a realistic diatom bond-length dependence for the H_2-rare gas dispersion coefficients, LeRoy et al. [9] approximated their linear stretching-dependence by those of the spherically averaged polarizability $\bar{\alpha}$ and polarizability anisotropy $\Delta\alpha$ of diatomic hydrogen: $d\ln(C_6^0)/dr = d\ln(\bar{\alpha})/dr$ and $d\ln(C_6^2)/dr = d\ln(\Delta\alpha)/dr$. The assumption that those logarithmic derivatives did *not* depend on the nature of the interaction partner was clearly only a first approximation, and later work showed that for rare gas partners, the first derivatives obtained in that way are ca. 50% too large [12, 18]. This motivated Thakkar [20] to calculate bounds to C_6^0 and C_6^2 for *atom* + H_2 interactions as a function of the H_2 bond length, using *ab initio* DOSD moments for H_2, H, and He, and semiempirical DOSD for other rare gas and alkali atoms. Those values [20] were then fitted to convenient r-expansions and incorporated into expressions for the overall potential energy surfaces for the H_2-rare gas systems [12, 18, 19, 21] which have since found widespread use.

In subsequent work, Tang and Toennies [22] combined Meyer's *ab initio* pseudo-DOSD for H_2 [15] with a semiempirical pseudo-DOSD for Ne to calculate C_6^0 and C_6^2 for H_2–Ne at three values of the H_2 bond length. Similarly, Matías and Varandas [23, 24] used Meyer's pseudo-DOSD for H_2 and *ab initio* and semiempirical pseudo-DOSD for a variety of atoms to compute C_6^0 and C_6^2 for *atom* + H_2 interactions at three different H_2 bond lengths. They also generated estimates of C_6^0 for *atom* + H_2 interactions at a range of H_2 bond lengths using simple Unsold and Kirkwood approximations based upon *ab initio* results for H_2, H and He, and semiempirical data for the other atoms [23, 24].

The present paper describes an improved version of the unpublished, although extensively used [12, 18, 19, 21], work of Ref. [20]. In particular, C_6^0 and C_6^2 coefficients for the interactions of H_2 with H, Li, Be, He, Ne, Ar, Kr and Xe are determined as functions of the H_2 bond length. Section 2 presents these results, together with a description of the methodology used to generate them. Section 3 then describes fits to these results to obtain compact analytic expressions which incorporate the H_2 bond-length dependence of these coefficients.

2. Dispersion coefficients for atom + H_2 interactions

2.1. Theory

The C_6 coefficient for the interaction between an S-state atom and a Σ-state diatomic molecule with bond length r may be written in two forms:

$$C_6(r,\theta) = C_6^0(r)[1 + \Gamma(r)P_2(\cos\theta)] = C_6^0(r) + C_6^2(r)P_2(\cos\theta) \qquad (2)$$

where $\Gamma(r) = C_6^2(r)/C_6^0(r)$. It is convenient [13–17, 25] to express the isotropic and anisotropic components of the dispersion coefficient, $C_6^0(r)$ and $C_6^2(r)$, in terms of the components $C_6^{\{110\}}(r)$ and $C_6^{\{111\}}(r)$ as:

$$C_6^0(r) = C_6^{\{110\}}(r) + 2C_6^{\{111\}}(r) \qquad (3)$$

and

$$C_6^2(r) = C_6^{\{110\}}(r) - C_6^{\{111\}}(r) \qquad (4)$$

For each value of the diatom bond length r, the isotropic or spherically-averaged dispersion coefficient may be expressed in terms of the frequency-dependent isotropic dipole polarizabilities of the diatom (here H_2) and the atom (denoted A) as [25–27]:

$$C_6^0 = \frac{3}{\pi}\int_0^\infty \alpha_{H_2}(i\omega)\alpha_A(i\omega)\,d\omega \qquad (5)$$

where $i = \sqrt{-1}$. Similarly, for $C_6^{\{110\}}(r)$ and $C_6^{\{111\}}(r)$ one may write:

$$C_6^x = \frac{1}{\pi}\int_0^\infty \alpha_{H_2}^x(i\omega)\alpha_A(i\omega)\,d\omega \quad \text{for } x = \{110\} \text{ or } \{111\} \qquad (6)$$

where $\alpha_{H_2}^{\{110\}}$ and $\alpha_{H_2}^{\{111\}}$ are, respectively, the $m = 0$ and $m = 1$ components of the dynamic dipole polarizability of the H_2 diatom [13–17, 25]. The dependence of the dispersion coefficients on the diatom bond length clearly arises from the bond-length dependence of these dynamic polarizabilities. In the present work, the requisite dynamic polarizabilities are approximated by pseudo-spectral expansions of the form:

$$\alpha(i\omega) = \sum_{j=1}^{N} g_j/[\omega_j^2 + \omega^2] \tag{7}$$

in which the pseudo-oscillator strengths g_j and the pseudo-excitation energies ω_j define the underlying pseudo-DOSD.

2.2. The pseudo dipole oscillator strength distributions

In the calculations reported below, nearly exact *ab initio* pseudo-DOSD were used for the H and He atoms. In particular, the 21-term pseudo-DOSD (i.e., Eq. (7) with $N = 21$) used for H is based on exact moments of the true DOSD, and yields a value for $C_6(\mathrm{H}+\mathrm{H})$ which is accurate to 15 significant figures [28]. Similarly, the 30-term pseudo-DOSD used for He was obtained by a variational perturbation calculation using Slater–Hylleraas geminals, and is known to yield a value for $C_6(\mathrm{He}+\mathrm{He})$ which is accurate to five significant figures [29].

For the Be atom, a reasonably accurate *ab initio* pseudo-DOSD was obtained using the relation:

$$\sum_{j=1}^{N} g_j \omega_j^k = S(k) \tag{8}$$

for selected values of k. The $S(k)$'s appearing here are moments of the true DOSD, defined by:

$$S(k) = \sum_{j=1}^{\infty} f_j \varepsilon_j^k + \int_{E_c}^{\infty} \varepsilon^k (df/d\varepsilon)\, d\varepsilon \tag{9}$$

where f_j and ε_j are the dipole oscillator strength and excitation energy for the transition between the ground and jth discrete excited state, $df/d\varepsilon$ is the density of the dipole oscillator strength for transitions into the continuum, and E_c is the continuum threshold energy. In the present work, the parameters defining a three-term pseudo-DOSD for Be were determined by applying Eq. (8) to *ab initio* $S(k)$ values for $-3 \leqslant k \leqslant 2$ obtained by a second-order polarization propagator calculation using a coupled cluster double excitation ansatz [30]. The value of $S(-2)$ used for Be is in excellent agreement with other high-accuracy *ab initio* calculations of its static dipole polarizability [31].

The ten-term semiempirical pseudo-DOSD used for Li [32] and for Ne, Ar, Kr, Xe [33] are expected to have accuracies of about 1%. Static dipole polarizabilities calculated from these semiempirical pseudo-DOSD are, respectively, 0.55%, 0.79%, 1.4%, 1.7% and 2.2% lower than the latest *ab initio* values for Li [34], Ne [35], Ar [36], Kr [37] and Xe [37]. An analysis of the residual errors in the calculations for Kr and Xe suggests that the *ab initio* polarizabilities have uncertainties of about 1% as well [37]. Thus, the pseudo-DOSD and *ab initio* polarizabilities agree within the mutual uncertainties. The situation is not altogether satisfactory because the pseudo-DOSD values are systematically lower than the *ab initio* ones, but we have little choice but to use the former.

To obtain pseudo-DOSD for H_2 at a range of bond lengths, we began with a compilation of *ab initio* oscillator strengths, excitation energies, and of the DOSD moments $S(k)$ for $-2 \leqslant k \leqslant 2$ [38, 39]. This compilation is based exclusively upon calculations employing wave functions constructed from James–Coolidge geminals [38, 39]. The values in the compilation are expected to be of very high accuracy, except for $S(2)$ at $r = 3.8$ and 4.0 a.u., for which an extrapolation was necessary [38]. In addition, values of $S(-3)$ for H_2 as a function of its bond length have been obtained by combining the compilation mentioned above with a novel sum-rule function which incorporates both the high-energy and resonance behaviours of the true DOSD [38, 39]. This compilation and set of $S(-3)$ values were then used to generate pseudo-DOSD for H_2 in the manner described below.

Three different isotropic pseudo-DOSD were used for H_2 at each bond length. The first two terms of each one were defined by the true oscillator strengths and excitation energies for vertical transitions between the ground and the two lowest discrete excited states of H_2. A four-term pseudo-DOSD, referred to as U, was then obtained by requiring it to also reproduce the $S(k)$'s for $-2 \leqslant k \leqslant 1$. Similarly, a five-term pseudo-DOSD, referred to as L, was obtained by requiring it to reproduce $S(k)$ for $-2 \leqslant k \leqslant 2$ and the true excitation energy for a transition between the ground and the third discrete excited state. Finally, another five-term pseudo-DOSD, referred to as E, was obtained by requiring it to reproduce $S(k)$ for $-3 \leqslant k \leqslant 2$. For the anisotropy, three-term longitudinal and transverse pseudo-DOSD's were obtained for H_2 by requiring them to reproduce the oscillator strengths for transitions from the ground to the lowest Σ and Π excited states, respectively, the excitation energies for the transitions from the ground to the two lowest Σ and Π excited states, and the $\{111\}$ and $\{110\}$ components of the moments $S(k)$ for $k = 0, -1, -2$.

2.3. *Results*

Table 1 presents three different values of C_6^0 for each *atom* + H_2 interaction, at sixteen H_2 bond lengths ranging from $r = 1$ to 4 a.u. The values with superscripts *UB* and *LB*, respectively, were obtained with the U and L pseudo-DOSD for H_2, while the third value was generated using the E pseudo-DOSD for H_2. The U and L pseudo-DOSD were constructed in a manner which would cause them to yield rigorous upper and lower bounds on C_6^0 if the atomic pseudo-DOSD were exact [40–42].

The condition that the atomic pseudo-DOSD be exact is essentially satisfied for the hydrogen and helium atoms, so our bounds for the H_2–H and H_2–He isotropic C_6 coefficients may be considered rigorous to the numbers of digits cited. For the other interactions, the atomic pseudo-DOSD have uncertainties of about 1% and the bounds are not rigorous at all. The results obtained with the E pseudo-DOSD should be the best, since they use the largest amount of H_2 data; however, the lower bound [40, 42] character of this pseudo-DOSD is nullified because we used approximate values [38, 39] of $S(-3)$. On the other hand, it is satisfying to note that these E-based estimates *always* lie between the (non-rigorous) "bounds", and that they also agree well with estimates (not shown) obtained from these bounds using the generalized mean technique [42]. Moreover, interpolation over these "best-estimate" results yields values of C_6^0 and Γ for $r = 1.28$, 1.449 and 1.618 a.u. which agree to

Table 1. Calculated upper bound $C_6^{0,UB}$, lower bound $C_6^{0,LB}$, and best-estimate isotropic C_6^0 coefficients, all in *atomic* units, and the best-estimate $P_2(\cos\theta)$ anisotropy coefficient $\Gamma = C_6^2/C_6^0$ for the systems of interest

	H_2–He				H_2–H				H_2–Li				H_2–Be			
r/a.u.	$C_6^{0,LB}$	$C_6^{0,UB}$	C_6^0	Γ	$C_6^{0,LB}$	$C_6^{0,UB}$	C_6^0	Γ	$C_6^{0,LB}$	$C_6^{0,UB}$	C_6^0	Γ	$C_6^{0,LB}$	$C_6^{0,UB}$	C_6^0	Γ
1.00	2.994	3.010	3.000	0.05763	6.302	6.341	6.318	0.06258	56.09	56.22	56.15	0.06787	30.71	30.86	30.78	0.06568
1.20	3.437	3.453	3.442	0.07432	7.366	7.406	7.382	0.08138	67.24	67.39	67.31	0.08957	36.40	36.56	36.47	0.08610
1.40	3.891	3.908	3.897	0.09086	8.482	8.525	8.498	0.1003	79.36	79.53	79.43	0.1122	42.49	42.66	42.56	0.1070
1.60	4.349	4.365	4.355	0.1066	9.628	9.673	9.647	0.1185	92.27	92.45	92.36	0.1344	48.86	49.04	48.94	0.1274
1.80	4.798	4.815	4.803	0.1212	10.78	10.82	10.79	0.1356	105.7	105.9	105.8	0.1560	55.35	55.55	55.43	0.1468
2.00	5.228	5.245	5.234	0.1345	11.89	11.94	11.91	0.1512	119.2	119.4	119.3	0.1761	61.78	61.99	61.88	0.1647
2.20	5.625	5.643	5.632	0.1458	12.94	12.99	12.96	0.1646	132.3	132.5	132.4	0.1941	67.93	68.15	68.03	0.1804
2.40	5.977	5.995	5.984	0.1547	13.89	13.94	13.91	0.1755	144.5	144.7	144.6	0.2094	73.55	73.79	73.66	0.1935
2.60	6.272	6.291	6.279	0.1610	14.69	14.75	14.71	0.1835	155.2	155.5	155.4	0.2213	78.41	78.67	78.53	0.2033
2.80	6.500	6.519	6.507	0.1641	15.32	15.38	15.34	0.1878	164.0	164.2	164.1	0.2291	82.29	82.56	82.42	0.2092
3.00	6.655	6.675	6.663	0.1638	15.75	15.82	15.78	0.1884	170.3	170.6	170.4	0.2325	85.03	85.32	85.17	0.2110
3.20	6.737	6.757	6.745	0.1602	15.99	16.06	16.02	0.1851	174.0	174.3	174.2	0.2311	86.58	86.88	86.74	0.2086
3.40	6.751	6.772	6.759	0.1534	16.04	16.11	16.07	0.1782	175.2	175.5	175.3	0.2251	87.00	87.30	87.16	0.2019
3.60	6.709	6.731	6.719	0.1439	15.94	16.01	15.97	0.1680	174.1	174.5	174.3	0.2148	86.43	86.75	86.61	0.1914
3.80	6.626	6.648	6.636	0.1322	15.72	15.79	15.76	0.1552	171.4	171.7	171.6	0.2007	85.15	85.48	85.34	0.1778
4.00	6.518	6.541	6.529	0.1191	15.43	15.50	15.47	0.1405	167.5	167.9	167.7	0.1838	83.38	83.73	83.59	0.1619

	H_2–Ne				H_2–Ar				H_2–Kr				H_2–Xe			
r/a.u.	$C_6^{0,LB}$	$C_6^{0,UB}$	C_6^0	Γ	$C_6^{0,LB}$	$C_6^{0,UB}$	C_6^0	Γ	$C_6^{0,LB}$	$C_6^{0,UB}$	C_6^0	Γ	$C_6^{0,LB}$	$C_6^{0,UB}$	C_6^0	Γ
1.00	6.088	6.117	6.098	0.05630	20.28	20.40	20.32	0.05974	28.78	28.96	28.85	0.06033	42.56	42.81	42.66	0.06107
1.20	6.961	6.990	6.971	0.07260	23.45	23.57	23.49	0.07731	33.36	33.54	33.43	0.07819	49.48	49.74	49.57	0.07928
1.40	7.855	7.884	7.865	0.08873	26.73	26.86	26.78	0.09482	38.12	38.30	38.19	0.09603	56.69	56.97	56.80	0.09756
1.60	8.753	8.782	8.763	0.1041	30.06	30.20	30.11	0.1116	42.96	43.15	43.04	0.1131	64.07	64.35	64.18	0.1151
1.80	9.632	9.662	9.642	0.1184	33.36	33.50	33.41	0.1271	47.77	47.96	47.84	0.1291	71.41	71.71	71.52	0.1315
2.00	10.47	10.50	10.48	0.1314	36.54	36.68	36.59	0.1413	52.41	52.61	52.49	0.1436	78.53	78.84	78.66	0.1465
2.20	11.25	11.28	11.26	0.1424	39.49	39.64	39.55	0.1534	56.73	56.95	56.82	0.1560	85.19	85.51	85.33	0.1594
2.40	11.93	11.96	11.94	0.1512	42.13	42.28	42.19	0.1632	60.60	60.82	60.69	0.1661	91.16	91.50	91.30	0.1698
2.60	12.51	12.54	12.52	0.1573	44.35	44.50	44.41	0.1701	63.86	64.09	63.96	0.1732	96.22	96.57	96.37	0.1773
2.80	12.95	12.98	12.96	0.1603	46.07	46.23	46.14	0.1736	66.41	66.64	66.51	0.1769	100.2	100.5	100.3	0.1813
3.00	13.25	13.29	13.26	0.1600	47.25	47.42	47.32	0.1737	68.15	68.40	68.26	0.1771	102.9	103.3	103.1	0.1817
3.20	13.41	13.44	13.42	0.1565	47.88	48.05	47.96	0.1702	69.09	69.35	69.20	0.1737	104.4	104.8	104.5	0.1784
3.40	13.44	13.47	13.45	0.1498	48.00	48.18	48.08	0.1633	69.28	69.54	69.39	0.1668	104.7	105.1	104.9	0.1715
3.60	13.35	13.39	13.37	0.1404	47.70	47.88	47.78	0.1534	68.83	69.11	68.96	0.1569	104.0	104.4	104.2	0.1615
3.80	13.19	13.23	13.21	0.1289	47.08	47.27	47.17	0.1412	67.93	68.21	68.07	0.1445	102.6	103.0	102.8	0.1489
4.00	12.98	13.02	13.00	0.1160	46.27	46.46	46.36	0.1275	66.73	67.02	66.88	0.1305	100.8	101.2	101.0	0.1347

Table 2. C_6 coefficients for *atom* + He systems, calculated as described in Sect. 2.2, expressed in atomic units

System	C_6/a.u.
He–H	2.821
He–He	1.461
He–Li	22.49
He–Be	12.92
He–Ne	3.032
He–Ar	9.551
He–Kr	13.42
He–Xe	19.57

better than 0.45% and 0.003 (or 2.9%), respectively, with values from Table 2 of Ref. [23].

3. Analytic representation of the angle and bond-length dependent C_6 coefficients

3.1. General

The previous section has presented upper and lower bounds on the values of $C_6^0(r)$ for a range of values of r, together with "best estimates" of both this quantity and of $\Gamma(r)$ at each H_2 bond length. The problem addressed here is that of devising accurate and compact representations of these coefficients for incorporation in overall potential energy surfaces for these systems.

In previous work [6, 9, 12, 19, 21], the diatom-stretching dependence of the $C_6^0(r)$ and $C_6^2(r)$ coefficients for the H_2-rare gas systems was represented by power series expansions in the Dunham coordinate $\xi = (r - r_0)/r_0$:

$$C_6^\lambda(r) = \sum_{k=0}^{k_{\max}} \xi^k C_6^{\lambda,k} \tag{10}$$

where r_0 is a suitably chosen reference length. Another possible choice for the expansion variable is one proposed by Ogilvie [43], $\zeta = (r - r_0)/(r + r_0)$, which is attractive because it maps the entire range of diatom internuclear separations from $r = 0$ to ∞ onto the finite range $\zeta = -1$ to $+1$. The practical utility of these two variables will be compared below. Note that in all cases considered herein, the reference length r_0 is defined as the expectation value of r for the ground vibration-rotation state of H_2, $r_0 = 0.7666393$ Å [44, 45].

In the limit when $r \rightarrow 0$, the electronic structure of an H_2 molecule becomes identical to that of a He atom. As a result, in this "collapsed diatom limit" the *atom* + H_2 interaction potentials become identical to the corresponding one-dimensional *atom* + He potential energy curves. In the present context, this means that as $r \rightarrow 0$, the $C_6^0(r)$ values must approach the C_6 coefficient for that atom interacting with He, while $C_6^2(r)$ must approach zero. LeRoy and Carley used the analytic form of Eq. (10) with $k_{\max} = 3$ to represent a less-accurate earlier set of $C_6(r, \theta)$ values [20], and incorporated the resulting $C_6^{\lambda,k}$ expansion coefficients into their diatom-stretching dependent H_2-rare gas potential energy surfaces [12, 18, 19]. They also introduced the use of *collapsed diatom limit* constraints for imposing the correct $r \rightarrow 0$ behaviour, in order to extend the range of diatom bond-lengths over which their interaction potentials were valid. Following their approach, we shall obtain $C_6^\lambda(r)$ functions which represent accurately the results presented in Table 1 and incorporate (see below) this physically-correct *collapsed diatom limit* behaviour.

3.2. The least-squares fits

We have performed least-squares fits of the best-estimate $C_6^0(r)$ and $C_6^2(r) = C_6^0(r) \times \Gamma(r)$ values from Table 1 to power series in the expansion variables ξ and ζ, while constraining the resulting functions to satisfy the collapsed diatom limit described above. For the isotropic terms $C_6^0(r)$, this constraint was implemented by simply including the C_6 coefficient for the corresponding *atom* + He interaction as a $\xi = -1$ or $\zeta = -1$ point in the data set. The C_6(*atom* + He) coefficients used for this purpose are listed in Table 2; they were computed from Eq. (5) using the atomic pseudo-DOSD discussed in Sect. 2.2, with the dynamic polarizability of H_2 replaced by that of He. For the anisotropic ($\lambda = 2$) dispersion coefficients, the collapsed diatom limit constraint takes on the form:

$$C_6^2(\xi = -1) = C_6^2(\zeta = -1) = \sum_{k=0}^{k_{\max}} (-1)^k C_6^{2,k} \equiv 0 \qquad (11)$$

This allows the leading coefficient of the power series expansion to be expressed in terms of the others:

$$C_6^{2,0} = \sum_{k=1}^{k_{\max}} (-1)^{k-1} C_6^{2,k} \qquad (12)$$

so that only $k_{\max}$ of these coefficients are really independent parameters.

As in any least-squares fitting procedure, each datum was weighted by the squared inverse of the associated uncertainty. For the isotropic components of the interaction between H_2 and H or He, the calculations are highly accurate, so the differences between the upper- and lower-bound values given in Table 1, $[C_6^{0,UB} - C_6^{0,LB}]$, are believed to provide realistic estimates of the uncertainties. However, the results for H_2 interacting with the other atoms are less accurate, and more realistic estimates of the uncertainties in those $C_6^0(r)$ values are believed to be ca. 1% of the best estimate for the given coefficient. Moreover, since the $S(2)$ moments for H_2 at the bond lengths $r = 3.8$ and 3.0 a.u. were obtained by extrapolation, the uncertainties associated with $C_6^0(r)$ at these two distances are set at twice the values which would have been assumed otherwise (i.e., $2 \times [C_6^{0,UB} - C_6^{0,LB}]$ for H and He, and 2% for the others). Finally, the uncertainties in the values of C_6(*atom* + He) which define the $C_6^0(r = 0)$ limits of the *atom* + H_2 interactions were assumed to be equal to the smallest of the uncertainties associated with the other $C_6^0(r)$ values for that case.

While we have no direct way of knowing the uncertainties in the $C_6^2(r)$ (or $\Gamma(r)$) values, estimates may be obtained using the interrelationships provided by Eqs. (3) and (4) and the definition $\Gamma(r)$. In particular, if we consider the $C_6^0(r)$ and $C_6^2(r)$ values at any given r to be functions of $C_6^{\{110\}}(r)$ and $C_6^{\{111\}}(r)$, and the uncertainties in the latter to be uncorrelated, the uncertainties in the former may be expressed as [46]:

$$u(C_6^\lambda(r)) = \left\{ \left[\frac{\partial C_6^\lambda(r)}{\partial C_6^{\{110\}}(r)} u(C_6^{\{110\}}(r)) \right]^2 + \left[\frac{\partial C_6^\lambda(r)}{\partial C_6^{\{111\}}(r)} u(C_6^{\{111\}}(r)) \right]^2 \right\}^{1/2} \tag{13}$$

for $\lambda = 0$ and 2. The partial derivatives appearing in Eq. (13) are readily obtained from Eqs. (3) and (4), and introduction of the assumption that $u(C_6^{\{110\}}(r)) \approx u(C_6^{\{111\}}(r))$ then yields the relationship:

$$u(C_6^2(r)) = \sqrt{2/5}\,u(C_6^0(r)) \tag{14}$$

In the fits reported below, the uncertainties used to weight the values of $C_6^2(r)$ obtained from the results in Table 1 were based on Eq. (14) and the $C_6^0(r)$ uncertainties described above.

Our final concern here is the selection of a criterion for determining the number of terms which should be included in the power series expansions of Eq. (10). To this end, we introduce a quantity called the "dimensionless standard error" or *DSE*:

$$DSE = \left\{ \left(\sum_{i=1}^{N_d} [Y_i(obs) - Y_i(calc)]^2 / u(Y_i)^2 \right) \Big/ [N_d - N_p] \right\}^{1/2} \tag{15}$$

where N_d is the number of data being fitted, N_p the number of parameters being varied, $Y_i(obs)$ the ith "experimental" datum, $u(Y_i)$ its uncertainty, and $Y_i(calc)$ is the value of it calculated from Eq. (10). A *DSE* value $\leqslant 1$ means that on average, the discrepancies between the input data and the predictions of the model are smaller than the uncertainty in the former, and hence that this model provides a satisfactory representation of those data. This criterion is used to determine the smallest values of $k_{\max}$ sufficient to provide accurate power series representations of the various $C_6^\lambda(r)$ functions.

3.3. Results

We begin by examining the question of whether the Dunham coordinate ξ or the Ogilvie coordinate ζ is the more convenient variable to use in the power series expansion of Eq. (10). Fits of the calculated $C_6^0(r)$ and $C_6^2(r)$ values for H_2–Ar

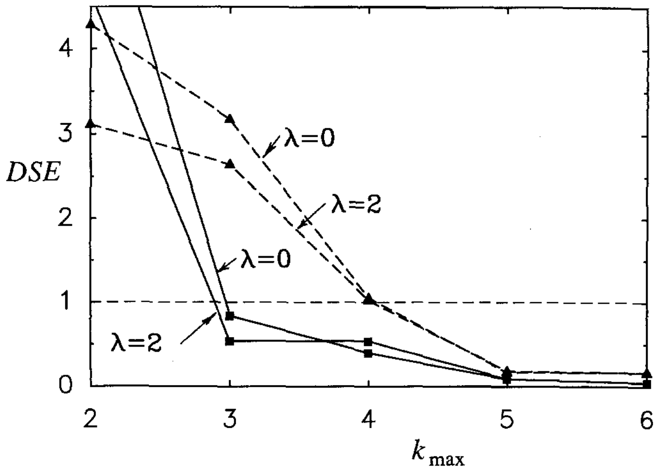

Fig. 1. *DSE* values for fits of power series of order $k_{\max}$ in the variable ξ (square points joined by *solid lines*) or ζ (triangular points joined by *broken lines*) to the H_2–Ar $C_6^\lambda(r)$ values of Table 1

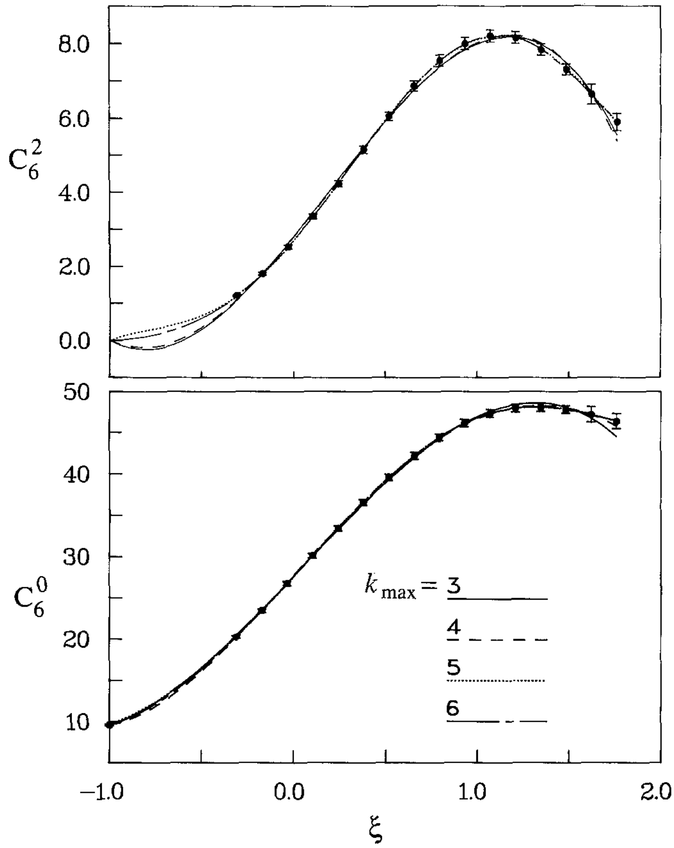

Fig. 2. Polynomials in ξ of order $k_{\max}$ obtained from least-squares fits to the $C_6^\lambda(r)$ values for H_2–Ar, for $\lambda = 0$ (*lower segment*), $\lambda = 2$ (*upper segment*); the ordinate scale is in atomic units. The points shown are the best-estimate values from Table 1 while the associated error bars indicate the uncertainties used to weight these points

to power series in ξ and ζ for a range of values of $k_{\max}$, subject to the collapsed diatom limit constraint of Eq. (12), yielded the *DSE* values shown in Fig. 1, while plots of the resulting polynomials are seen in Figs. 2 and 3. Figure 1 clearly shows that when the Ogilvie coordinate ζ is used (triangular points joined by dashed lines), much higher values of $k_{\max}$ are required to achieve good fits. Moreover, Fig. 3 shows that expansions in ζ are much more likely to show implausible oscillations in the broad interpolation region between the calculated values at $r = 1$ a.u. ($\xi = -0.31$ or $\zeta = -0.18$) and the collapsed diatom limit at $\xi = \zeta = -1$. Similar results were obtained for other systems. Thus, the Dunham coordinate $\xi = (r - r_0)/r_0$ is clearly the better variable for polynomial expansion representations of the $C_6^\lambda(r)$ functions.

For a range of $k_{\max}$ values, the best-estimate results for all of the cases considered in Table 1 were fitted to the ξ expansions of Eq. (10), while applying the collapsed diatom limit constraints described above. The *DSE* values for those fits are plotted vs. $k_{\max}$ in Fig. 4, while plots of the associated polynomials for three representative cases are compared with the input $C_6^\lambda(r)$ values in Figs. 2, 5 and 6. In each case, the optimum polynomial representation corresponds to the smallest value of $k_{\max}$ for which the $DSE < 1$.

The results in Fig. 4 show that these systems may be divided into three groups: (i) H_2 with H and He, (ii) H_2 with Ne, Ar, Kr and Xe, and (iii) H_2 with

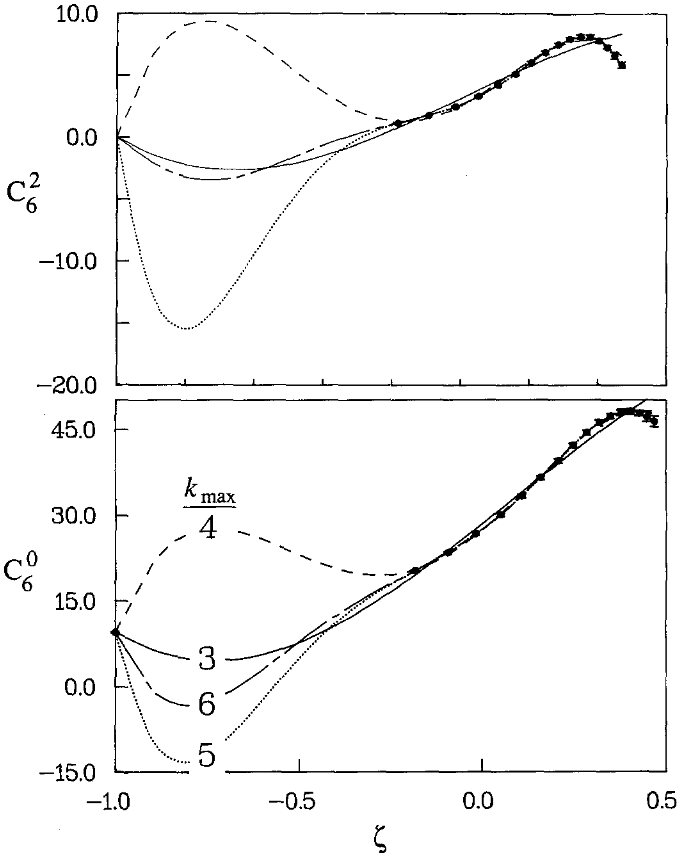

Fig. 3. As in Fig. 2, for polynomials in ζ

Li and Be. For systems in group (ii), cubic functions of ξ (corresponding to $k_{max} = 3$) yield *DSE* values less than 1 for both $\lambda = 0$ and 2. In contrast, the relatively small uncertainties associated with the calculated $C_6^\lambda(r)$ values for H_2–H and He mean that adequate polynomial representations are not obtained until $k_{max} = 5$. The group (iii) systems are intermediate cases in which $k_{max} = 3$ suffices for the $C_6^0(r)$ expansion, but $k_{max} = 4$ is required for $C_6^2(r)$.

Figures 2, 5 and 6 show that the $k_{max} = 3$ and 4 curves for $\lambda = 2$ all have negative slopes at the collapsed diatom limit point $\xi = -1$, and that the corresponding $k_{max} = 5$ curves have an inflection point in the broad small-r interpolation region. Adoption of the $k_{max} = 6$ polynomials would eliminate this somewhat unlikely behaviour. However, it would significantly increase the complexity of our expressions for $C_6^2(r)$, and since we know of no physical arguments forbidding a local maximum or minimum in this region, we prefer the more compact (small k_{max}) representations suggested by Fig. 4.

In general, the numbers of digits used to represent parameter values determined from a least-squares fit should be the minimum number sufficient to "adequately" represent the input data. Moreover, the requisite numbers of significant digits may be further reduced if one exploits the interparameter correlation by using a sequence of additional fits, in each of which one additional

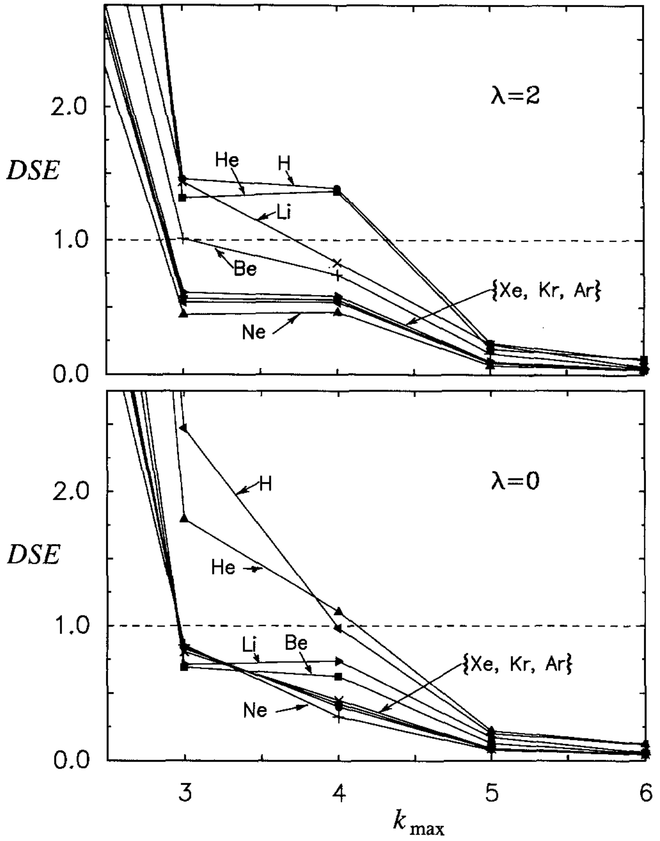

Fig. 4. *DSE* values for fits of Eq. (10) to the data of Table 1 for various values of k_{max}: *lower segment* – for $\lambda = 0$, *upper segment* – for $\lambda = 2$

parameter is held fixed at the rounded-off value suggested by the preceding fit [47]. We have used a successive-rounding scheme of this type to determine our final recommended values for the expansion parameters $C_6^{\lambda,k}$ of Eq. (10) [48]. The resulting recommended values of these expansion coefficients for all of the systems of interest are presented in Table 3. Note that although the results being fitted to (see Table 1) were originally calculated in atomic units, prior to determining these expansion coefficients they were converted to the units $\text{cm}^{-1}\,\text{Å}^6$ more commonly used for representing model potential functions (with conversion factors taken from Ref. [49]).

4. Concluding remarks

We report accurate new values of the isotropic and $P_2(\cos\theta)$ anisotropy dispersion coefficients for diatomic hydrogen interacting with H, Li, Be and the rare gases, which explicitly take account of their dependence on the diatom bond length r. Compact polynomial representations of these r-dependent coefficients were also determined, in order to facilitate their incorporation in three-dimensional model potential energy surfaces for these systems.

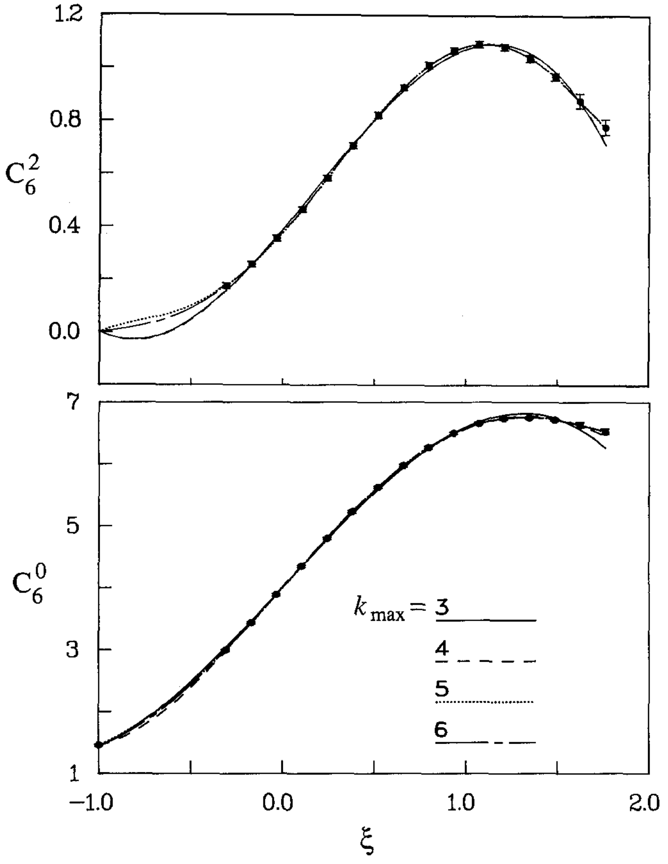

Fig. 5. For H_2–He, as in Fig. 2

The expansions obtained on substituting the coefficients of Table 3 into Eq. (10) accurately represent the diatom-stretching dependence of the C_6 coefficients for H_2 interacting with a range of partners. However, when calculating spectroscopic properties or collision cross sections for these systems, one usually needs to know the diagonal or off-diagonal vibrationally-averaged values of these coefficients. Such averages may be readily generated by replacing the powers of ξ in Eq. (10) by the associated diagonal or off-diagonal vibrational matrix elements of ξ^k for the vibration-rotation states in question. For example, the vibrationally-averaged C_6 value associated with the interaction of H_2 in vibration-rotation state (v, j) with a chosen atom may be written as:

$$\bar{C}_6^{\lambda}(v,j) = \sum_{k=0}^{k_{max}} \langle v,j|\xi^k|v,j\rangle C_6^{\lambda,k} \qquad (16)$$

Accurate values of the requisite expectation values of powers of ξ are readily obtained from tabulated results for all vibration-rotation states of all six isotopomers of H_2 [44].

A comparison of the utility of the Dunham ($\xi = [r - r_0]/r_0$) and Ogilvie ($\zeta = [r - r_0]/[r + r_0]$) stretching coordinates in power series representation of these $C_6^{\lambda}(r)$ values shows that the latter are much less useful than the former. The reason for this seems to be the fact that mapping the region from r_0 to ∞ onto

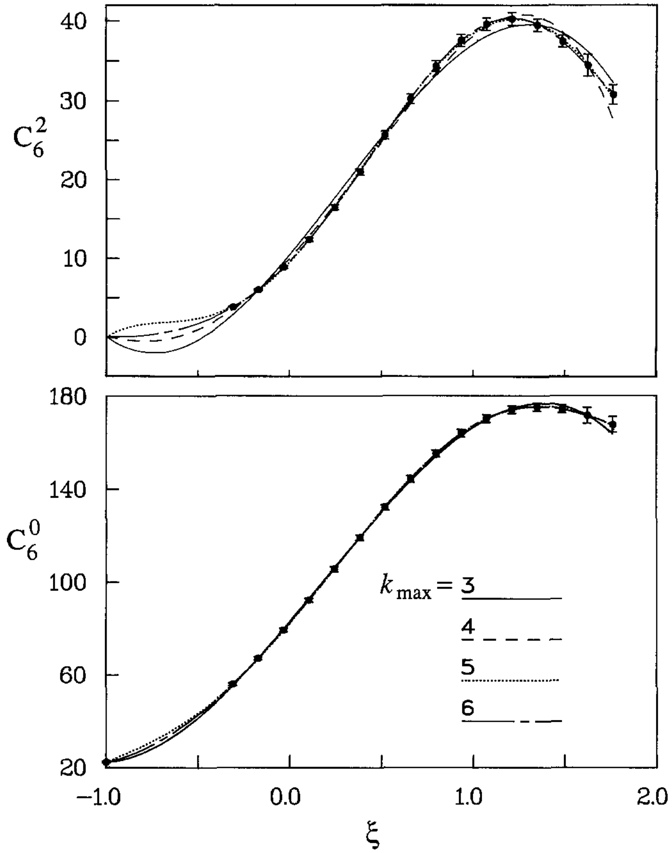

Fig. 6. For H_2–Li, as in Fig. 2

the finite range [0, 1] attempts to compress too broad a range of behaviour onto a narrow interval, and hence requires the use of much higher-order polynomials than desired. In our case, this also gives rise to implausible oscillations of the resulting $C_6^2(r)$ functions at small values of ζ (see Fig. 3). Thus, we conclude that at least for systems involving molecular hydrogen, the Ogilvie parameter ζ is much less useful than the traditional Dunham parameter ξ in providing convenient and stable representations of the internal bond-length dependence of intermolecular potential energy surfaces.

While the present paper has addressed the problem of determining and representing stretching-dependent C_6 dispersion coefficients for a variety of H_2 + atom systems, they are, of course, only one component of the overall potential energy surfaces for these systems. Unfortunately, it is much more difficult to generate analogous theoretical estimates of contributions such as the higher-order inverse-power terms in the long-range potential, the short-range repulsion, or even the electron overlap induced damping of the R^{-6} dispersion term. The higher-order and short-range terms are relatively stronger, and will have more overt effects on experimental data. However, if reliable estimates of the overall potential energy surfaces are to be obtained from fits to such data, it is necessary to minimize the model-dependence of the analysis by defining as precisely as possible the asymptotically-dominant dispersion term. This has been the problem addressed by the present work.

Table 3. Coefficeints $C_6^{\lambda,k}$ defining the recommended polynomial representations of $C_6^{\lambda}(\xi)$ (see Eq. (10)) for H_2 interacting with various atoms. Their units, cm^{-1} Å^6, are related to the atomic units of the input results from Table 1 by the conversion factor 4819.38157 [49], while the reference length appearing in the definition of the expansion variable $\xi = (r - r_0)/r_0$ is $r_0 = 0.7666393$ Å [44]

System	*DSE*	$C_6^{0,0}$	$C_6^{0,1}$	$C_6^{0,2}$	$C_6^{0,3}$	$C_6^{0,4}$	$C_6^{0,5}$
$H-H_2$	0.22	42236	40120	4080	−11100	−2000	1700
$He-H_2$	0.20	19298	16080	440	−4254	−340	530
$Ne-H_2$	0.86	38900	30500	100	−6000		
$Ar-H_2$	0.84	133000	113600	3000	−23400		
$Kr-H_2$	0.83	189700	165300	5500	−34500		
$Xe-H_2$	0.81	282500	252000	10000	−53000		
$Li-H_2$	0.72	400700	454000	55000	−107000		
$Be-H_2$	0.69	213300	221000	19600	−50000		
		$C_6^{2,0}$	$C_6^{2,1}$	$C_6^{2,2}$	$C_6^{2,3}$	$C_6^{2,4}$	$C_6^{2,5}$
$H-H_2$	0.24	4400	9970	5620	−4250	−2960	1340
$He-H_2$	0.19	1816	3791	1730	−1655	−940	470
$Ne-H_2$	0.45	3720	7720	1300	−2700		
$Ar-H_2$	0.54	13600	29700	5700	−10400		
$Kr-H_2$	0.57	19700	43600	8600	−15300		
$Xe-H_2$	0.61	29900	67900	14000	−24000		
$Li-H_2$	0.84	48700	121700	58000	−30000	−15000	
$Be-H_2$	0.75	24600	59100	22500	−17000	−5000	

Acknowledgements. This research has been supported by the Natural Sciences and Engineering Research Council of Canada and by the Centres of Excellence for Molecular and Interfacial Dynamics, and C.E.C. is pleased to acknowledge the support provided by an Ontario Graduate Scholarship. In addition, A.J.T. is grateful to Prof. W.C. Nieuwpoort of the University of Groningen for his hospitality during the time this paper was being written.

References and notes

1. See, e.g., (a) Hirschfelder JO, Curtiss CF, Bird RB (1964) Molecular theory of gases, liquids. Wiley, New York; (b) Hirschfelder JO, Meath WJ (1967) The nature of intermolecular forces. In: Hirschfelder JO (ed) Adv Chem Phys 12 (Intermolecular Forces), pp 3–106
2. Maitland GC, Rigby M, Smith EB, Wakeham WA (1981) Intermolecular forces: Their origin, determination. Clarendon Press, Oxford
3. Indeed, the only quantitative way of determining them appears to be from analysis of the spectroscopic properties of discrete vibrational levels lying near the dissociation threshold [4], or from the use of oscillator strength sums [5]. However, the former approach is only appropriate for atom + atom interactions, and the latter for isotropic and vibrationally-averaged (over any internal degrees of freedom) values
4. (a) LeRoy RJ (1974) Can J Phys 52:246; (b) LeRoy RJ (1980) J Chem Phys 73:6003; (c) Gerstenkorn S, Luc P, Amiot C (1985) J Phys France 46:355; (d) Davies MR, Shelley JC, LeRoy RJ (1991) J Chem Phys 94:3479
5. (a) Zeiss GD, Meath WJ (1977) Mol Phys 33:1155; (b) Margoliash DJ, Meath WJ (1978) J Chem Phys 68:1246; (c) Jhanwar BL, Meath WJ (1980) Mol Phys 41:1061; (d) Meath WJ, Margoliash DL, Jhanwar BL, Kiode A, Zeiss GD (1981) Accurate molecular properties, their additivity, and their use in constructing intermolecular potentials. In: Pullman B (ed), Intermolecular Forces (Proceedings of the 14th Jerusalem Symposium on Quantum Chemistry and Biochemistry) pp 101–115
6. LeRoy RJ, Van Kranendonk J (1974) J Chem Phys 61:4750

7. McKeller ARW, Welsh HL (1971) J Chem Phys 55:595
8. Rulis AM, Smith KM, Scoles G (1978) Can J Phys 56:753
9. LeRoy RJ, Carley JS, Grabenstetter JE, (1977) Faraday Disc Chem Soc 62 (Potential Energy Surfaces):169
10. Toennies JP, Welz W, Wolf G (1976) J Chem Phys 64:5305
11. Toennies JP, Welz W, Wolf G (1979) J Chem Phys 71:614
12. LeRoy RJ, Carley JS (1980) Spectroscopy and potential energy surfaces of Van der Waals molecules. In: Lawley KP (ed) Adv Chem Phys 42 (Potential Energy Surfaces), pp 353–420
13. (a) Victor GA, Dalgarno A (1970) J Chem Phys 53:1316; (b) Victor GA, Slavsky DB (1974) J Chem Phys 61:3484
14. Langhoff PW, Gordon RG, Karplus M (1971) J Chem Phys 55:2126
15. Meyer W (1976) Chem Phys 17:27
16. Meyer W, Hariharan PC, Kutzelnigg W (1980) J Chem Phys 73:1880
17. Thakkar AJ (1977) Chem Phys Lett 46:453
18. Carley JS (1978) PhD Thesis, University of Waterloo
19. LeRoy RJ (1984) Chapter 13 in Resonances in Electron-Molecule Scattering, Van der Waals Complexes and Reactive Chemical Dynamics, Truhlar DG (ed), ACS Symposium Series, No 263, American Chemical Society, pp 231–262
20. Thakkar AJ (1977) unpublished paper presented at the 6th Canadian Symposium on Theoretical Chemistry, Fredericton, New Brunswick
21. LeRoy RJ, Hutson JM (1987) J Chem Phys 86:837
22. Tang KT, Toennies JP (1982) J Chem Phys 76:2524
23. Matías MA, Varandas AJC (1990) Mol Phys 70:623
24. Varandas AJC, Matías MA (1988) Chem Phys Lett 148:149
25. Mulder F, van Dijk G, van der Avoird A (1980) Mol Phys 39:407
26. Dalgarno A (1967) New methods for calculating long-range intermolecular forces, in: Hirschfelder JO (ed) Adv Chem Phys 12 (Intermolecular Forces), pp 143–166
27. Buckingham AD (1967) Permanent and induced molecular moments and long-range intermolecular forces, in: Hirschfelder JO (ed) Adv Chem Phys 12 (Intermolecular Forces), pp 107–142
28. Thakkar AJ (1988) J Chem Phys 89:2092
29. Thakkar AJ (1981) J Chem Phys 75:4496
30. Oddershede J, Sabin JR (1989) Phys Rev A39:5565
31. Thakkar AJ (1989) Phys Rev A40:1130
32. Margoliash DJ, Meath WJ (1978) J Chem Phys 68:1426
33. Kumar A, Meath WJ (1985) Mol Phys 54:823
34. Maroulis G, Thakkar AJ (1989) J Phys B22:2439
35. (a) Taylor PR, Lee TJ, Rice JE, Almlöf J (1989) Chem Phys Lett 163:359; (b) Maroulis G, Thakkar AJ (1989) Chem Phys Lett 156:87
36. Cernusak I, Diercksen GHF, Sadlej AJ (1986) Chem Phys Lett 128:18
37. Maroulis G, Thakkar AJ (1988) J Chem Phys 89:7320
38. Hu Z-M (1990) MSc Thesis, University of New Brunswick
39. Hu Z-M, Thakkar AJ (1990) to be published
40. Luyckx R, Delbaen F, Coulon Ph, Lekkerkerker HNW (1979) Phys Rev A19:324
41. Langhoff PW (1971) Chem Phys Lett 12:217
42. Thakkar AJ (1984) J Chem Phys 81:1919
43. (a) Ogilvie JF (1974) Report on Flexible Potential Energy Functions, Australian National University Research School of Chemistry; (b) Ogilvie JF (1981) Proc R Soc Lond A378:287; (c) ibid (1982) A381:479
44. (a) Schwartz C, LeRoy RJ (1987) J Mol Spectrosc 121:420; (b) Le Roy RJ, Schwartz C (1987) Univ. of Waterloo Chemical Physics Research Report CP-301R
45. This choice of r_0 means that the expectation value of ξ will be identically zero for the ground state of the most common isotope of the diatom [6]
46. Taylor JR (1982) An introduction to error analysis, University Science Books, Mill Valley, CA
47. Tellinghuisen J (1989) J Mol Spectrosc 137:248
48. In this procedure, the rounding was stopped if the sum of squares of deviations between the calculated, observed quantities became more than 2% larger than its optimal value
49. Cohen ER, Taylor BN (1987) Rev Mod Phys 59:1121